SCIENTIFIC REPORTS

OPEN

SUBJECT AREAS:
TRANSLATIONAL RESEARCH
CANCER THERAPEUTIC RESISTANCE

Received
14 March 2014

Accepted
18 June 2014

Published
4 July 2014

Correspondence and requests for materials should be addressed to J.W. (JWang4@mdanderson.org)

Distinguishing between cancer cell differentiation and resistance induced by all-trans retinoic acid using transcriptional profiles and functional pathway analysis

Song-Mei Liu[1], Weiping Chen[2] & Jin Wang[3]

[1]Center for Gene Diagnosis, Zhongnan Hospital of Wuhan University, Wuhan, Hubei 430071, China, [2]Microarray Core, National Institute of Diabetes and Digestive and Kidney Diseases, National Institutes of Health, Bethesda, MD 20892, USA, [3]Department of Translational Molecular Pathology, The University of Texas, M.D. Anderson Cancer Center, Houston, TX 77030, USA.

All-trans retinoic acid (*ATRA*) induces differentiation in various cell types and has been investigated extensively for its effective use in cancer prevention and treatment. Relapsed or refractory disease that is resistant to *ATRA* is a clinically significant problem. To identify the molecular mechanism that bridges *ATRA* differentiation and resistance in cancer, we selected the multidrug-resistant leukemia cell line HL-60[R] by exposing it to *ATRA*, followed by sequential increases of one-half log concentration. A cytotoxicity analysis revealed that HL-60[R] cells were highly resistant to *ATRA*, doxorubicin, and etoposide. A comparative genome hybridization analysis of HL-60[R] cells identified gains of *4q34*, *9q12*, and *19q13* and a loss of *Yq12* compared with in the parental HL-60 cell line. Transcriptional profiles and functional pathway analyses further demonstrated that 7 genes (*FEN1*, *RFC5*, *EXO1*, *XRCC5*, *PARP1*, *POLR2F*, and *GTF2H3*) that were relatively up-regulated in HL-60[R] cells and repressed in cells with *ATRA*-induced differentiation were related to mismatch repair in eukaryotes, DNA double-strand break repair, and nucleotide excision repair pathways. Our results suggest that transcriptional time series profiles and a functional pathway analysis of drug resistance and *ATRA*-induced cell differentiation will be useful for identifying promyelocytic leukemia patients who are eligible for new therapeutic strategies.

The leukemia from which the human HL-60 cell line was derived was classified in 1976 as acute progranulocytic leukemia (APL) and had several atypical features[1–3]; it has been used extensively as an *in vitro* model for studying cell growth and differentiation. In the presence of all trans-retinoic acid (*ATRA*), HL-60 cells undergo myeloid differentiation, which involves reorganization of the nucleus and cytoplasm, migration, and eventual apoptosis[4]. *ATRA* treatment was also found to increase APL cells' adhesion and invasion capabilities[5]. Previous studies have focused on the nuclear and cytoskeletal changes and the kinetics of protein changes in HL-60 cells with *ATRA*-induced differentiation[6,7]. A high proportion of patients with APL experience complete remission after treatment with *ATRA*[8–10]; however, continuous treatment causes a progressive reduction in plasma drug concentrations, which can cause clinical relapse and *ATRA* resistance[11].

To overcome these pharmacologic effects and understand the molecular mechanisms of drug resistance so that we can initiate large-scale studies of chronic treatment with *ATRA* in patients with APL, we selected multi-drug-resistant (MDR) HL-60[R] cells from those that had been exposed to 10 nM *ATRA* after being treated with 1.0 μM *ATRA* for 6 days, followed by sequential increases of one-half log concentration every 2 weeks. Some retardation of growth, attended by the presence of a variable fraction of differentiated cells, was noted from inception, as determined using Gallagher's method[12]. This was most marked at 1.0 μM *ATRA*; at this concentration, a progressively expanding cell population formed in 3 months. The HL-60[R] cells were maintained at an *ATRA* concentration of 1.0 μM for 6 months. A bioactivity analysis showed that the cells were about 120 times more resistant to *ATRA* than were the parental cells. We collected all the RNA samples, from HL-60 cells with differentiation induced by 1.0 μM *ATRA* for 2 days, 4 days, and 6 days to *MDR* HL-60[R] cells with *ATRA*

selected for 1 month, 3 months, and 6 months, and analyzed their transcriptional time series profiles, which would be undertaken to comprehensively identify defects acquired in *ATRA* resistance and the *ATRA*-induced cell differentiation response by identifying pathways that are commonly deregulated during drug resistance.

Results

Cytotoxicity analysis of resistant HL-60[R] cells and HL-60 cells using MTT and cell cycle assays. Resistant HL-60[R] cells were derived from their parental HL-60 cells that had been treated with stepwise increasing concentrations of *ATRA* and maintained in 1.0 μM *ATRA* for 6 months. The cytotoxicities of *ATRA*, doxorubicin (*Dox*), and *VP-16* (etoposide) were determined in *MDR* HL-60[R] cells and drug-sensitive parental HL-60 cells. *MDR* HL-60[R] cells were highly resistant to *ATRA*, doxorubicin, and *VP-16* (Fig. 1A and B), with lethal doses (IC_{50}) of 24.61 μM, 3.02 μM, and 3.12 μM, respectively. On the other hand, the IC_{50} of HL-60 cells treated with *ATRA*, doxorubicin, and *VP-16* were 0.20 μM, 0.22 μM, and 0.12 μM, respectively (Fig. 1C–E and Table 1). *ATRA* had significant effects on HL-60 cells, and these changes in cell growth also determined the percentage of cells that were arrested at the *G1/G0* phase of the cell cycle (Fig. 1F and G). However, HL-60[R] cells were not arrested at *G1/G0* after 1.0 μM *ATRA* treatment (Fig. 1H) because of their resistance.

CGH studies of chromosomal gains, losses, and amplifications in HL-60[R] cells. The CGH results of *MDR* HL-60[R] and HL-60 cells, including 1 example of a CGH ratio profile, are shown in Fig. 2; genetic imbalances were present in HL-60 and *MDR* HL-60[R] cells. We identified 4 genetic changes in the *MDR* HL-60[R] cell line, including 1 loss (*Yq12*) and 3 gains (*4q34*, *9q12*, and *19q13*), compared with in its parental HL-60 cell line. We also confirmed that *ZNF230*, *NUP62*, *E2-EPF*, and *CNOT3*, which are located in *19q13*, were up-regulated in *MDR* HL-60[R] cells compared to in their parental HL-60 cells (Table S1).

Hierarchical cluster analysis of differentially expressed genes regulated by *ATRA* treatment in resistant HL-60[R] and parental HL-60 cells. Using a hierarchical clustering analysis, we compared the similarities in the expression patterns of the 210 differentially expressed genes, which were differentially expressed in more than 3 samples at 7 time points (HL-60 cells treated with 1.0 μM *ATRA* for 2 days, 4 days, or 6 days and HL-60[R] cells maintained with 1.0 μM *ATRA* for 1 month, 3 months, or 6 months, compared to their parental HL-60 cells). A more than 2.0-fold change in the transcription level was used as the cut-off value for identifying the differentially expressed genes. The dendrogram, part of which is shown in Figure 3, demonstrates the relationships between genes, as calculated by the clustering algorithm. A gradual change over the 7 time points was observed after treatment with *ATRA*. The genes could be divided into 4 clusters. Cluster A included those genes for which mRNA levels peaked at day 2 of treatment (Fig. 3, Cluster A), including 10 ribosomal protein genes (*RPL23A*, *RPL38*, *RPS28*, *RPL3*, *RPLP1*, *RPL23*, *RPL11*, *RPL19*, *RPL13A*, and *RPS24*) and 2 eukaryotic translation elongation factors (*EEF1G* and *EEF2*) that were up-regulated by *ATRA* treatment (80.0% of genes in Cluster A). These genes were involved in protein synthesis and metabolism. Cluster B included genes that were expressed maximally at day 4 or day 6 (Fig. 3, Cluster B); these were biomarkers of differentiation, such as known *ATRA* differentiation molecules (*JWA*, *ARPC3*, *TMSB10*, *TXNIP*, and *DEFA1*) and *CD* antigens (*CD4* and *CD63*)[4]. Cluster C included genes for which mRNA levels increased after ATRA treatment at 1 month, 3 months, or 6 months (*OARS*, *TNRC1*, *HNRPA1*, *SNRPB*, *PAICS*, *MLC1SA*, *HNRPK*, *E2-EPF*, *CTSC*, *NUP62*, *POH1*, *COX4I1*, *ZNF230*, *SF3B2*, *ERP70*, *CNOT3*, and *MAP2K4*). Cluster D included genes for which mRNA levels increased gradually over the treatment time course and were expressed maximally at 6 months (*PLA2G1B*, *ARHGD1B*, *ACAT1*, *NCL*, *UOCRH*, *PPIB*, *GPI*, *DACH*, *PTDSS1*, *PSMD8*, *ODC1*, *TAGLN2*, *HRMT1L2*, and *PKBP1A*) (Fig. 3, Cluster D). These genes are related to DNA repair, cell survival, metabolism, and drug resistance and were over-expressed in *MDR* HL-60[R] cells.

Gene expression profiles in *MDR* HL-60[R] and HL-60 cells with *ATRA*-induced differentiation. The gene expression profiles of *MDR* HL-60R cells were compared to those of parental HL-60 cells. A more than 2.0-fold change in the transcription level was used as the cut-off value to identify the differentially expressed genes ($p \leq 0.05$). We found that compared to their parental HL-60 cells, 104 genes were relatively up-regulated in *ATRA*-resistant HL-60[R] cells and repressed in cells with *ATRA*-induced differentiation; 69 genes were relatively repressed in HL-60[R] and up-regulated in differentiated HL-60 cells; 6 genes (*IFNGR1*, *TGIF*, *SPAG9*, *CSF2RB*, *LRRFIP1*, and *SLC21A3*) were up-regulated in both resistant and differentiated cells; and 20 genes were repressed in both resistant and differentiated cells (Table S1). The over-expressed genes in *MDR* HL-60[R] are related to DNA repair, stress response, drug resistance, the ubiquitin-proteasome pathway, and protein synthesis and metabolism, including anti-oxidation, oxidative phosphorylation, and the mitochondrial pathway.

Functional networks and pathways of *ATRA*-induced drug resistance were analyzed by the IPA. The genetic networks and cellular pathways were derived using the IPA program by analyzing 104 genes that were up-regulated in *ATRA*-resistant HL-60[R] cells. A more comprehensive network and pathway analysis of all deregulated genes revealed their association with 3 important network functions and 5 critical canonical pathways, all of which are relevant to the development of *ATRA*-resistant cancer. The differently expressed genes constituted about half the total molecules involved and the network-associated cellular functions and include those related to RNA post-transcriptional modification; DNA replication, recombination, and repair; cell death and survival; lipid metabolism; molecular transport; developmental disorders; hereditary disorders; and metabolic disease in resistant HL-60[R] cells (Table 2). These genes are expected to be affected in HL-60[R] cells. They belong to 5 canonical signaling pathways that are commonly deregulated in *ATRA* resistance (Table 3). Although only 10 (*FEN1*, *RFC5*, *EXO1*, *XRCC5*, *PARP1*, *NME1*, *SET*, *TSTA3*, *POLR2F*, and *GTF2H3*) were up-regulated in HL-60[R] cells and repressed in *ATRA*-induced differentiated cells with the signaling pathways (eukaryote mismatch repair, DNA double-strand break repair, granzyme A signaling, *GDP-L*-fucose biosynthesis I, and the nucleotide excision repair pathway), each has documented functions in controlling cell growth, and the DNA repair pathway has been implicated to play roles in *ATRA*-resistant HL-60[R] cells.

Discussion

We challenged the *MDR* cancer cells in our study with retinoic acid, doxorubicin and found that they involved the activation of different mechanisms of drug metabolism and were dependent on the bioactivities of certain cancer cell lines. *ATRA* is known to induce the *in vitro* and *in vivo* differentiation of APL cells and favor their release from the bone marrow into the blood at the initiation of therapy. In the presence of *ATRA*, HL-60 human promyelocytic cells underwent myeloid differentiation. *MDR* HL-60[R] cells, which were highly resistant to *ATRA*, did not undergo cell differentiation. We demonstrated that *MDR* HL-60[R] cells were more than 122-, 12-, and 25-fold resistant to *ATRA*, doxorubicin, and *VP-16*, respectively, compared to parental HL-60 cells (Table 1). In addition, cell cycle

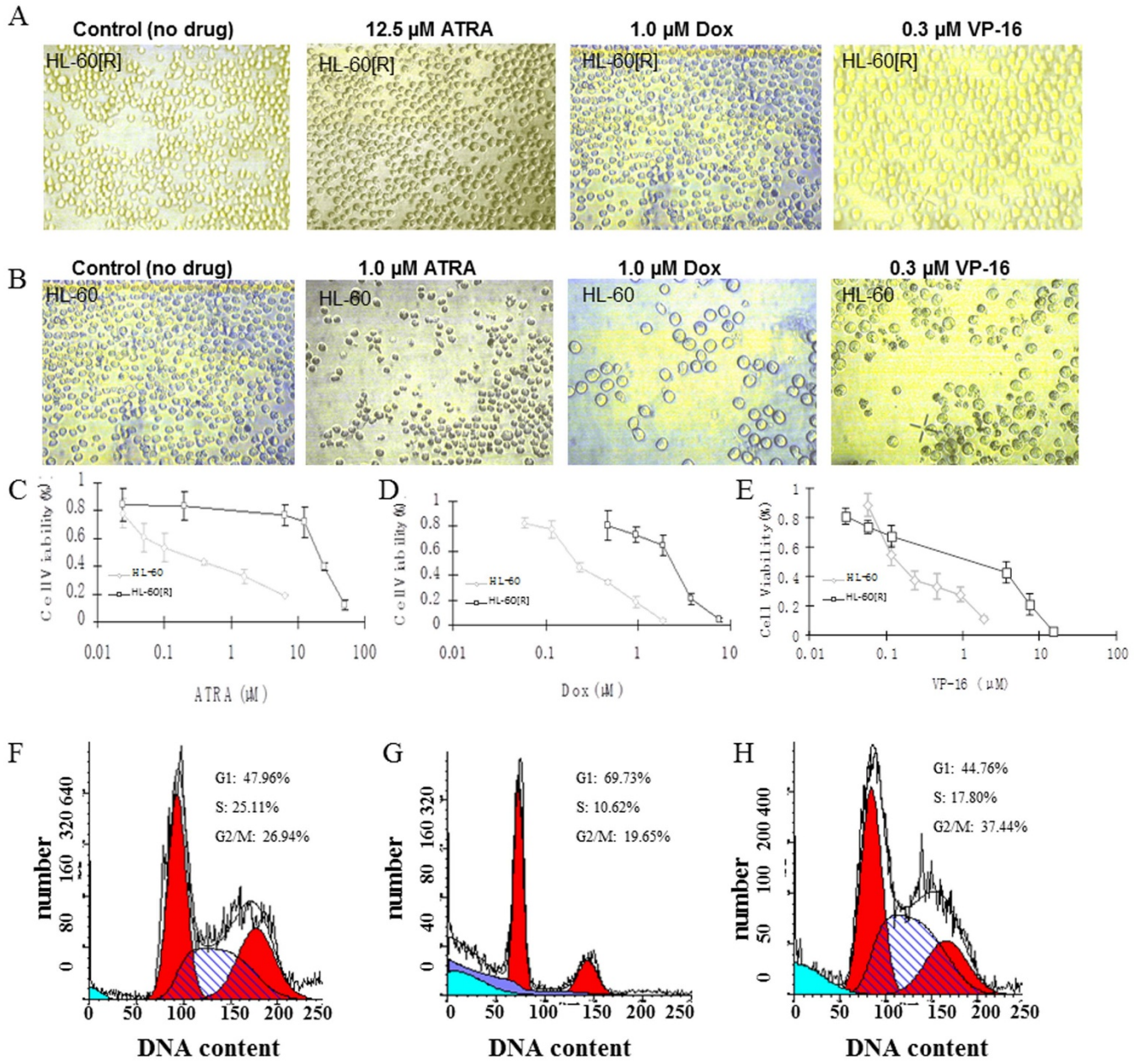

Figure 1 | **Cytotoxicity and flow cytometry analysis of HL-60[R] and HL-60 cells treated with 3 drugs (*ATRA*, doxorubicin [*Dox*], and *VP-16*).** (A) HL-60[R] cells treated with 12.5 μM *ATRA*, 1.0 μM doxorubicin, and 0.3 μM *VP-16*. (B) HL-60 cells treated with 1.0 μM *ATRA*, 1.0 μM doxorubicin, and 0.3 μM *VP-16*. Percentage of HL-60 and HL-60[R] cell viability after *ATRA* (C), doxorubicin (D), and *VP-16* (E) treatment, as determined by MTT assay. Flow cytometry analysis of the effect of *ATRA* on the cellular DNA content of HL-60 and HL-60[R] cells. (F) HL-60 cells without *ATRA*. (G) HL-60 treated with 1.0 μM *ATRA*. (H) *MDR* HL-60[R] cells maintained in 1.0 μM *ATRA*.

arrest was not induced at the *G1/G0* phase of the cell cycle in HL-60[R] cells but was induced in parental HL-60 cells with 1.0 μM *ATRA* treatment. Next, a CGH analysis of *MDR* HL-60[R] cells identified gains of *4q34*, *9q12*, and *19q13* and a loss of *Yq12* as the most prominent alterations compared with in parental HL-60 cells. It is well recognized that resistant cells with genetic alterations possess a growth or survival advantage that leads to clonal expansion. To understand the molecular mechanism by which *MDR* is induced by *ATRA* in HL-60[R] cells, we used a DNA microarray to monitor the changeable gene expression profiles, from the cell differentiation induced by *ATRA* to the development of *MDR*; we also analyzed the functional networks and pathways of *ATRA*-induced cell differentiation and drug resistance.

Table 1 | Cytotoxicity studies on HL-60 and HL-60[R] cells by MTT assay (IC_{50})

	HL-60	HL-60[R]	
Drug	IC_{50}	IC_{50}	Resistance index[a]
ATRA	0.20 μM	24.61 μM	123.05
Dox	0.22 μM	3.02 μM	13.73
VP-16	0.12 μM	3.12 μM	26.00

[a]Resistance index, ratio between the IC50 value of MDR HL-60[R] and parental HL-60 cells.

Chromosomal *19q13* has been reported to contain several genes that are important in DNA repair–specifically, nucleotide excision repair and apoptosis mechanisms such as *XPD*, *ERCC1*, and *RAI*. The *19q13* chromosomal region is important in cancer[13]. Our microarray analysis revealed that genes in the *19q13* chromosomal region–*ZNF230*, *NUP62*, *E2-EPF*, and *CNOT3*–were constitutively

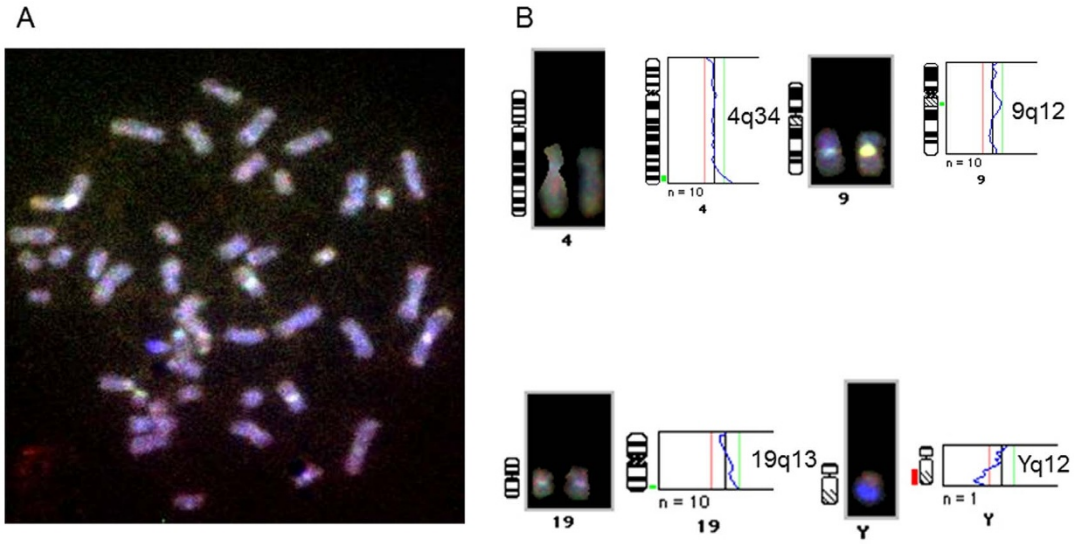

Figure 2 | CGH analysis of *MDR* HL-60[R] and HL-60 cell lines. (A) Representative image of CGH: *MDR* HL-60[R] to HL-60, (HL-60[R] labeled [spectrum green]/HL-60 labeled [spectrum red]). (B) CGH analysis shows that HL-60[R] cells have 3 chromosomal gains (*4q34*, *9q12*, and *19q13*) and 1 chromosomal loss (*Yq12*) compared with parental HL-60 cells.

over-expressed in *MDR* HL-60[R] cells (Table S1 and Fig. 3C). *NUP62* is an essential component of the nuclear pore complex and plays a novel role in centrosome integrity. Knockdown of *NUP62* induced *G2/M* phase arrest, mitotic cell death, and aberrant centrosome and centriole formation[14]. *E2-EPF*, named *UBE2S* (ubiquitin-conjugating enzyme *E2S*), accepts ubiquitin from the *E1* complex and catalyzes its covalent attachment to other proteins before elongating ubiquitin chains on *APC/C* substrates to promote mitotic exit[15]. High expression of *E2-EPF* was indicative of poor overall survival in a large-scale co-expression analysis of breast cancer[16]. It is interesting that *CNOT3* has also been associated with transcription regulation and represents a novel component of the core self-renewal and pluripotency circuitry that is conserved in mouse and human embryonic stem cells with *CNOT1* and *CNOT2*[17]. The chromosomal gene set enrichment analysis further confirmed that genes located at *19q13* were expressed at higher levels in uterine carcinosarcoma and contributed to its poor prognosis because of its epithelial-to-mesenchymal transition characteristics[18].

In our microarray, many genes involved in the retinoic acid signaling pathway (such as *RARRES2*, *CRABP2*, *MYC*, *TGIF*, *SUPV3L1*, *SET*, *ILF2*, *PTPRCAP*, *GPRK6*, and *SEC4L*) were up-regulated in *MDR* HL-60[R] cells. In previous studies, *RARRES2* (retinoic acid receptor responder 2 or chemerin) was over-expressed in malignant mesothelioma cells[19] and adrenocortical tumors[20] and was a biomarker for insulin resistance in type 2 diabetes mellitus patients[21]. *TGIF* functions as a transcriptional co-repressor and regulates developmental signaling by retinoic acid; it may also repress other *RXR*-dependent transcriptional responses[22]. Moreover, *TGIF*'s levels are inversely correlated with survival in patients with acute myelogenous leukemia, and its knockdown inhibits the differentiation of myeloid cell lines and increases apoptosis[23,24]. On the other hand, retinoic acid-resistant neuroblastoma cell lines also showed over-expression of *MYC* with *ATRA* in culture medium[25], and *SET* (*SET* nuclear oncogene), a potential marker for HNSCC that is associated with drug resistance, is up-regulated in 97% of tumor tissue samples and HNSCC cell lineages[26].

Next, we found that the genes involved in oxidative phosphorylation and metabolism (*ACAT1*, *ATP5G3*, *ARF4L*, *HEAB*, *PDHA1*, and *GNPI*) were differentially expressed in HL-60[R] cells; other genes involved in protein synthesis metabolism, such as eukaryotic translation initiation factors (*EIF2S1* and *EIF3S9*), transcription and elongation factors (*GTF3A*, *CNOT3*, *RUNX1*, and *TCEA1*), and splicing factors (*SFRS3* and *SFRS10*), were also over-expressed in MDR HL-60[R] cells. *ACAT1* expression may be a prognostic marker in prostate cancer: it was expressed at a significantly higher level in cancerous cores than in adjacent benign cores and was specifically effective at differentiating between indolent and aggressive forms of cancer[27]. Moreover, targeting *ACAT1* with avasimibe (*ACAT* inhibitor) could be an efficient treatment for glioblastoma because it can inhibit *ACAT1* expression and induce cell apoptosis[28]. The expression of *ARF4L* (adenosine diphosphate-ribosylation factor 4-like), a glioma-associated antigen, is controlled by the activated *Akt/mTOR* pathway, which is a downstream effect of the loss of *PTEN*[29]. *HEAB* (cleavage and polyadenylation factor I subunit 1) is a protein-coding gene that contains an adenosine triphosphate/guanosine triphosphate-binding motif that is homologous to the adenosine triphosphate-binding transporter superfamily or guanosine triphosphate-binding proteins[30]. *RUNX1* may play a critical role in chemotherapy response in acute megakaryocytic leukemia by regulating the phosphoinositide 3-kinase/*Akt* pathway[31], and ectopic *RUNX* reduces intracellular long-chain ceramides in NIH3T3 fibroblasts and elevated extracellular sphingosine 1 phosphate. *RUNX* expression also opposed the activation of *c-Jun-NH(2)*-kinase and *p38* (mitogen-activated protein kinase) and suppressed the onset of apoptosis in response to exogenous tumor necrosis factor α[32]. *SFRS3* (*SRp20*) is a serine- and arginine-rich splicing factor and proto-oncogene that is critical for cell proliferation and tumor induction and maintenance. Increased expression of *SFRS3* in rodent fibroblasts promoted immortal cell growth and transformation[33]. However, depletion of *SFRS10* resulted in apoptosis of the neural progenitor cells as well as disorganization of the cortical plate[34].

It is interesting that many of the genes related to DNA repair and cell survival (*NME1, DDX1*, *YWHAQ*, *PSMC1*, *PSMB6*, *E2-EPF*, *FEN1*, *RFC5*, *EXO1*, *UNG*, *XRCC5*, *ADPRT*, *POLR2F*, *Rpo1-2*, and *GTF2H3*) are over-expressed in *MDR* HL-60[R] cells. Of note, *POLR2F*, *XRCC5*, and *NME1* were reported to be repressed in retinoid-induced cell differentiation[4]. Most of these genes are related to mismatch repair in eukaryotes (*FEN1*, *RFC5*, and *EXO1*), DNA double-strand break repair (*XRCC5* and *PARP1*), and the nucleotide excision repair pathway (*POLR2F* and *GTF2H3*) on IPA analysis, and they are commonly up-regulated in *ATRA*-resistant HL-60[R] cells. Among these DNA repair genes, *FEN1* (Flap endonuclease 1) is

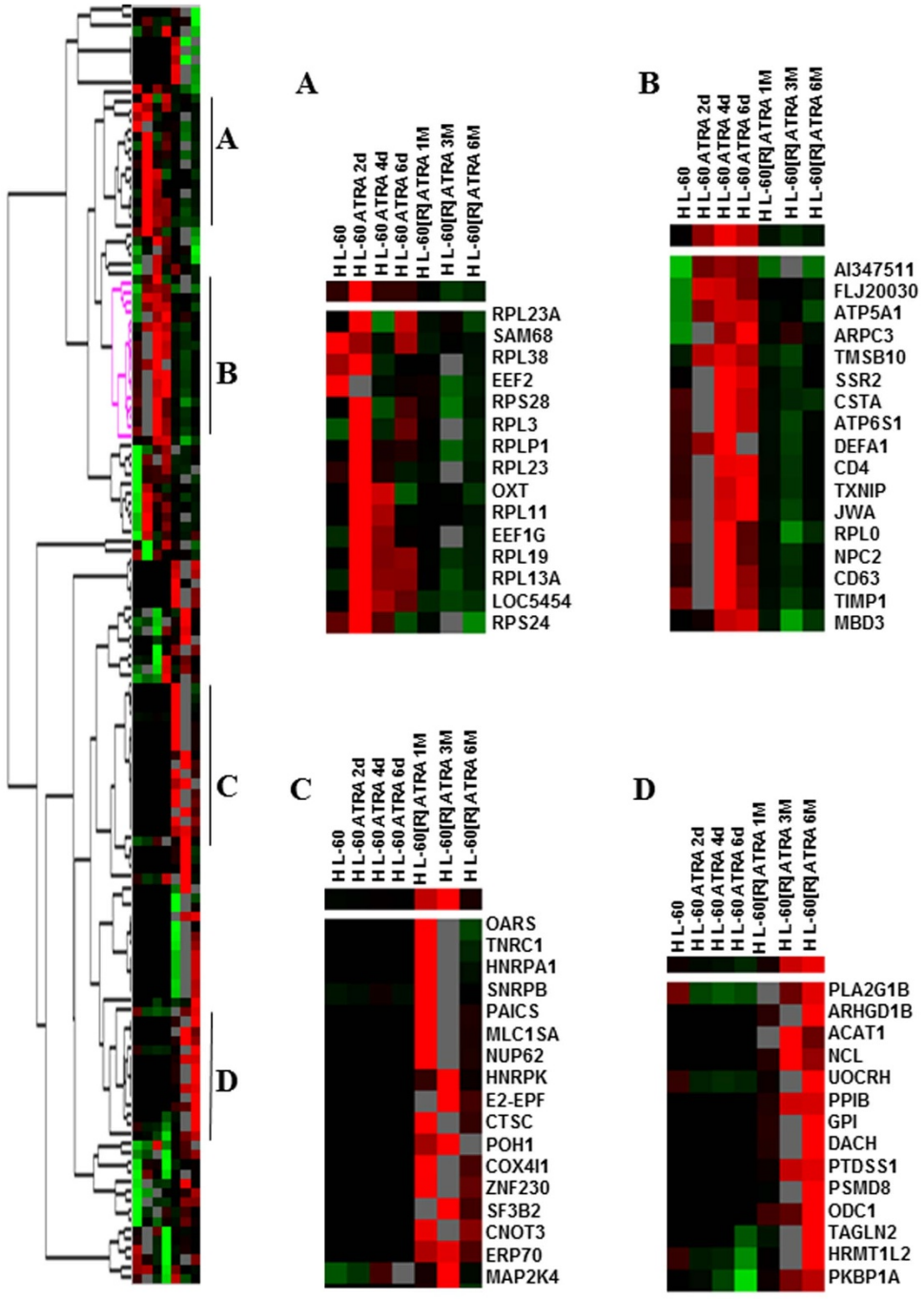

Figure 3 | Cluster image demonstrating different classes of gene expression profiles in HL-60 and HL-60[R] cells after *ATRA* treatment. We selected 210 genes whose RNA levels changed in response to 1.0 μM *ATRA* in HL-60 and HL-60[R] cells. (A) Cluster genes for which mRNA levels peaked at day 2 of *ATRA* treatment; (B) cluster genes that were expressed maximally at day 4 or day 6 of *ATRA* treatment; (C) cluster genes for which mRNA levels increased the *ATRA* treatment at 1 month, 3 months, or 6 months; and (D) cluster genes for which mRNA levels increased gradually over the *ATRA* treatment time course and were expressed maximally at 6 months.

a highly conserved structure-specific nuclease that catalyzes a specific incision to remove 5′ flaps in double-stranded DNA substrates; it plays an essential role in key cellular processes, such as DNA replication, repair, and mutation[35]. *ADPRT* (*PARP1*) is a critical DNA repair enzyme that is involved in DNA single-strand break repair via the base excision repair pathway. *PARP* inhibitors have been shown to sensitize tumors to DNA-damaging agents and selectively kill BRCA-deficient cancers[36,37]. *XRCC5* (*X-Ray* repair complementing defective repair in Chinese hamster cells 5) was over-expressed in cisplatin-resistant ovarian cancer cell lines[38]; it also affected chemosensitivity[39] and was associated with the *MDR* phenotype[40]. An immunohistochemical analysis verified significant co-expression of *MDR1* and *NME1* in human epithelial ovarian carcinoma[41]. Increased *NME1* mRNA levels were associated with resistance to initial chemotherapy in acute monocytic leukemia[42] and helped cells become resistant to oxidative stress[43]. On the other hand, higher levels of *UNG* (uracil-DNA glycosylase) were associated with pemetrexed resistance, and induction of *UNG* protein confirmed that up-regulation of the base excision repair enzyme is a feature of acquired pemetrexed resistance[44]. *DDX1* is a member of the *DEAD*

Table 2 | Genetic networks associated with *ATRA*-induced cell differentiation and drug resistance

Top 3 ATRA networks	Score	Focus molecules	Molecules in network
Resistance			
RNA post-transcriptional modification; DNA replication, recombination, and repair; cell death and survival	55	24	Akt, CD3, **CD14**, Ck2, **CLK2**, **CLNS1A**, **CSTF2**, **CTDP1**, cytochrome C, **DDX1**, **EXO1**, **GTF2H3**, histone h3, Holo RNA polymerase II, Hsp70, Hsp90, **HSPA4**, IFN β, **ILF2**, **NME1**, **PI4KB**, **POLR2F**, **POLR3F**, **PRMT5**, RNA polymerase II, **SRPK1**, **SRSF3**, **TCEA1**, **TRA2B**, **TRAP1**, **TSTA3**, ubiquitin, **VDAC2**, **XRCC5**, **YWHAQ**
DNA replication, recombination, and repair; lipid metabolism; molecular transport	43	20	26s proteasome, caspase, Cg, **CRABP2**, cyclin A, **DUSP3**, **EIF2S1**, **EIF3B**, ERK1/2, **FEN1**, GM-CSF, **GRK6**, Igm, Ikβ, **LAMP2**, Lh, **LIG1**, MAP2K1/2, Mek, **MMRN1**, **NFYA**, **PARP1**, **PEBP1**, **PSMB6**, **PSMC1**, **PTPRCAP**, Rar, Rfc, **RFC5**, **RUNX**1, **SCARB1**, Sos, TCR, **TMPO**, **UNG**
Developmental disorder, hereditary disorder, metabolic disease	30	15	**ADSL**, **ARL4D**, **ATP5G3**, CAND2, **CNOT3**, CNOT10, CNOT11, DENND4A, **DFNA5**, DRG2, EML4, **GBF1**, **GNPDA1**, GNPDA2, MAN1B1, **MTRR**, **MYO1D**, PCBD1, **PCK2**, **PGM1**, RAVER1, RNF38, **RNF114**, RNF219, **SEC62**, SEC63, SPG21, **SUPV3L1**, TBCE, TMEM230, TNKS1BP1, TRIM52, UBC, UEVLD, **ZNF263**
Differentiation			
Cellular compromise, developmental disorder, hereditary disorder	48	21	Actin, **ALB**, Ap1, **APOC2**, CD3, **CORT**, **DTNA**, **EIF2S1**, ERK1/2, F actin, **FBN1**, **FGR**, **FHL3**, growth hormone, insulin, **KLK7**, **KLKB1**, laminin, LDL, Lh, MAP2K1/2, Mlc, **MSMO1**, **MYO5A**, **NID1**, **NPPA**, **PAK1**, PI3K (complex), **POU2F1**, **PRKG1**, **RAB27A**, **SLC12A7**, **STX6**, TGFβ, **TXNIP**
Small molecule biochemistry, neurological disease, cell death and survival	44	19	Acot1, **ACOT8**, **AMY2B**, ARMCX5, ATF5, β-estradiol, **CLCA1**, **CLPTM1**, DDIT4, DHCR7, FOS, **H1FX**, HTT, IL2RB, **KCNAB2**, **MAN1A2**, MST1R, **NAP1L3**, NEDD9, **PET112**, **PLXNB3**, **REST**, **SLCO2B1**, **SPOCK1**, **ST8SIA5**, **STEAP1**, THRSP, TNF, TP73, **TXNIP**, UBC, **VASH1**, **VEZF1**, **ZNF217**, ZNF616
Infectious disease, cellular movement, hematological system development and function	17	9	26s proteasome, **ACO1**, adenosine, Akt, **APC**, **CEACAM6**, ERK, F2RL1, **FOXF1**, **GLS**, GOT, IFN, IgG, IL-1, IL-12 (complex), IL2RB, IL3RA, interferon alpha, Jnk, KISS1, **LTB**, MAP3K8, Mapk, **MYD88**, NADPH oxidase, NF-κB (complex), NLRP3, NOX4, P38 MAPK, Pkc(s), Ras, **STC2**, **TRAP1**, uric acid, VEGF

box protein family, which has *RNase* activity, plays an RNA clearance role at DNA double-strand break sites, and facilitates the template-guided repair of transcriptionally active regions of the genome[45].

We also demonstrated that about 69 genes, including *MYO5A*, *PAK1*, *FGR*, *PET112*, *GLS*, *ALB*, *MYD88*, *APOC2*, and *KLKB1*, were up-regulated in HL-60 cells treated with *ATRA* and were repressed in HL-60[R] cells. The genes in cells with *ATRA*-induced differentiation were involved in cellular compromise, developmental and hereditary disorders, small molecule biochemistry, cell death and survival, cellular movement, hematological system development, and functional networks (Table 2). Next, we found that *ATRA* induced cell differentiation via pathways, including *FcY* receptor-mediated phagocytosis in macrophages and monocytes (*MYO5A*, *PAK1*, and *FGR*), L-glutamine biosynthesis II (*PET112*), glutamine degradation I (*GLS*), interleukin-12 signaling and production in macrophages (*ALB*, *MYD88*, and *APOC2*), and acute-phase response signaling pathways (*KLKB1*, *ALB*, and *MYD88*) (Table 3). These functional networks and pathways will help us understand the disease response to retinoic acid's biological effects in promyelocytic leukemia chemotherapy.

In summary, in this study, we characterized the genes that are involved in DNA repair and cell survival, oxidative phosphorylation and metabolism, and the retinoic acid signaling pathways in *ATRA*-resistant HL-60[R] cells; we further revealed novel coordinated changes that occurred in resistant cells that allowed them to survive the cell differentiation and apoptosis elicited by *ATRA* chemotherapy. Thus, it is possible that blocking DNA repair and cell survival signaling pathways will not only enhance *ATRA* chemotherapy and improve the outcomes of patients with APL but also reduce the risk of second primary tumors.

Methods

Human myeloid leukemia HL-60 and HL-60[R] cell lines. The HL-60 cells were maintained in RPMI 1640 medium (Life Technologies, Inc.) containing 10% fetal calf serum, with penicillin, streptomycin, and glutamine added in a 5% CO_2 humidified atmosphere at 37°C. The cultures were initiated at a density of 0.2×10^6 cells/ml in 10-ml cultures every 2 days. *ATRA* was added separately from 1.0 mM stock that had

Table 3 | Top 5 canonical pathways involving genes that are differently expressed in ATRA- differentiated HL-60 and -resistant HL-60[R] cells, as determined by Ingenuity Pathway Analysis

Top 5 *ATRA* pathways	p value	Ratio	Molecules
Resistance			
Mismatch repair in eukaryotes	4.75E-05	1.25E-01	FEN1, RFC5, EXO1
DNA double-strand break repair	1.77E-03	1.00E-01	XRCC5, PARP1
Granzyme A signaling	3.27E-03	1.00E-01	NME1, SET
GDP-L-fucose biosynthesis I	9.00E-03	1.43E-01	TSTA3
Nucleotide excision repair pathway	1.09E-02	5.56E-02	POLR2F, GTF2H3
Differentiation			
FcY receptor-mediated phagocytosis in macrophages and monocytes	2.01E-03	2.83E-02	MYO5A, PAK1, FGR
L-glutamine biosynthesis II (tRNA-dependent)	5.38E-03	9.09E-02	PET112
Glutamine degradation I	5.38E-03	2.00E-01	GLS
IL-12 signaling and production in macrophages	5.63E-03	1.91E-02	ALB, MYD88, APOC2
Acute phase response signaling	1.06E-02	1.66E-02	KLKB1, ALB, MYD88

been dissolved in ethanol, stored away from light at −20°C, and used at a final concentration of 1.0 μM. The HL-60[R] cells were maintained with 1.0 μM *ATRA*.

Cytotoxicity assay. We performed an MTT (3-(4,5 dimethylthiazol-2-yl)-2,5 tetrazolium bromide) assay, which is based on the enzymatic (mitochondrial dehydrogenase) reduction of the tetrazolium salt, MTT, to a colored formazan product by viable cells[46]. Cells were plated in 96-well microassay culture plates at a cell density of 10^4 cells/well and grown overnight at 37°C in a 5% CO_2 incubator. Test compounds were then added to the wells to achieve a final concentration of 10^{-6} to 10^{-4} M. Control wells were prepared by adding 100 μl of culture medium with no cells. The plates were incubated at 37°C in a 5% CO_2 incubator for 72 h, and 20 μl of the stock MTT dye solution (5 mg/ml) was added to each well. After 4 h of incubation, 100 μl of DMSO was added to solubilize the MTT formazan. The optical density of each well was then measured with a microplate spectrophotometer at a wavelength of 570 nm. The IC_{50} was determined from the plots of the percentage viability vs. the dose of compound added.

Cell cycle analysis. To determine the cell cycle distribution, we plated 0.2×10^6 HL-60 and HL-60[R] cells in 60-mm dishes and treated them separately with 1.0 μM *ATRA* for 2 days. Cells were then collected and fixed in 95% ethanol, washed in 1% bovine serum albumin and phosphate-buffered saline, resuspended in 1.0 g/ml *RNase* and 50 μg/ml propidium iodide, incubated for 30 min in the dark at 37°C, and analyzed by flow cytometry using FACSCalibur. The data were analyzed using the ModFit DNA analysis program.

Comparative genomic hybridization and digital image analysis. Comparative genomic hybridization (CGH) was performed essentially as described previously[47,48]. The genomic DNA was prepared from HL-60 and HL-60[R] cells using the DNA Isolation Kit for Cells and Tissues (Boehringer Mannheim Corp., Indianapolis, IN, USA), according to the manufacturer's instructions. Slides were counterstained with DAPI and mounted with anti-fading solution (Vectashield; Vector, Burlingame, CA). CGH was performed using a digital image analysis system that contained a Zeiss Axioplan 2 microscope equipped with a Sensys cooled-charged device camera (Photometrics, Ltd., Tucson, AZ, USA), as previously described[48]. High copy number amplification of a chromosomal region was defined as a tumor : reference or HL-60[R] : HL-60 ratio of 1 : 50.

RNA extraction and gene expression profiling. RNA was isolated with Trizol LS (Invitrogen, Carlsbad, CA, USA) and purified using the RNeasy Mini Kit (Qiagen, Valencia, CA, USA). RNA quality was assessed using an Agilent 2100 Bioanalyzer (Agilent Technologies, Waldbronn, DE, USA). Microarray experiments were carried out using whole human genome oligonucleotide arrays with 20 μg of total RNA starting material, according to the manufacturer's protocol (National Cancer Institute [NCI] array). Total RNA from each sample was synthesized into double-stranded cDNA with SIII reverse transcriptase (Invitrogen) using an oligonucleotide d(T) primer. The double-stranded cDNA from HL-60 cells was labeled with Cy3 monofunctional reactive dye (Amersham Biosciences), and that from HL-60 [R] cells or *ATRA*-treated HL-60 cells was labeled with Cy5 monofunctional reactive dye (Amersham Biosciences). The probe was hybridized to an NCI oligonucleotide array (Hs-Operon V3-v1p24.gal) containing 36 K human transcripts (NCI Microarray Facility, Advanced Technology Center, Gaithersburg, MD) overnight at 42°C. For each treatment, the arrays were also queried with probes produced via reverse labeling, and the data were consistent with those obtained with initial standard labeling. Microarray slides were scanned with a GenePix 4000B microarray scanner (Axon Instruments, Union City, CA).

Microarray data and pathway analysis. The microarray images were analyzed with GenePix 5.1 software, and the subsequent gene lists and associated expression values were loaded into mAdb (NCI Microarray Facility). Fluorescence ratios were normalized for each array using a single scaling factor so that the median fluorescence ratio of well-measured spots on each array was 1.0. After flagging the bad spots, the mean $\log_2$-transformed ratio of resistant versus sensitive cells was calculated from triplicate experiments. The mean data were calculated using the antilog as the ratio of gene expression measures of resistant cells to parental cells and analyzed using Partek Genomics Solution software, as reported in our previous studies[49]. To determine the specific pathways on the basis of changes in gene expression, we used the Ingenuity Pathway Analysis (IPA) (http://www.ingenuity.com) commercial gene pathway analysis web tool.

Statistical analysis. All statistical values are presented as means ± S.D. Data were analyzed using Student's *t*-test. The results were considered significant at $p < 0.05$.

1. Collins, S. J., Gallo, R. C. & Gallagher, R. E. Continuous growth and differentiation of human myeloid leukaemic cells in suspension culture. *Nature* **270**, 347–349 (1977).
2. Collins, S. J., Ruscetti, F. W., Gallagher, R. E. & Gallo, R. C. Terminal differentiation of human promyelocytic leukemia cells induced by dimethyl sulfoxide and other polar compounds. *Proc. Natl. Acad. Sci. U. S. A.* **75**, 2458–2462 (1978).
3. Dalton, W. T., Jr. *et al.* HL-60 cell line was derived from a patient with FAB-M2 and not FAB-M3. *Blood* **71**, 242–247 (1988).
4. Wang, J. *et al.* Gene expression analysis of human promyelocytic leukemia HL-60 cell differentiation and cytotoxicity induced by natural and synthetic retinoids. *Life Sci.* **84**, 576–583 (2009).
5. Ovcharenko, A., Granot, G., Shpilberg, O. & Raanani, P. Retinoic acid induces adhesion and migration in NB4 cells through Pyk2 signaling. *Leuk. Res.* **37**, 956–962 (2013).
6. Olins, A. L., Buendia, B., Herrmann, H., Lichter, P. & Olins, D. E. Retinoic acid induction of nuclear envelope-limited chromatin sheets in HL-60. *Exp. Cell Res.* **245**, 91–104 (1998).
7. Olins, A. L. *et al.* Nuclear envelope and chromatin compositional differences comparing undifferentiated and retinoic acid- and phorbol ester-treated HL-60 cells. *Exp. Cell Res.* **268**, 115–127 (2001).
8. Huang, M. E. *et al.* Use of all-trans retinoic acid in the treatment of acute promyelocytic leukemia. *Blood* **72**, 567–572 (1988).
9. Castaigne, S. *et al.* All-Trans Retinoic Acid as a Differentiation Therapy for Acute Promyelocytic Leukemia .1. Clinical-Results. *Blood* **76**, 1704–1709 (1990).
10. Warrell, R. P., Jr. *et al.* Differentiation therapy of acute promyelocytic leukemia with tretinoin (all-trans-retinoic acid). *N. Engl. J. Med.* **324**, 1385–1393 (1991).
11. Muindi, J. *et al.* Continuous treatment with all-trans retinoic acid causes a progressive reduction in plasma drug concentrations: implications for relapse and retinoid "resistance" in patients with acute promyelocytic leukemia. *Blood* **79**, 299–303 (1992).
12. Gallagher, R. E. *et al.* Characterization of differentiation-inducer-resistant HL-60 cells. *Leuk. Res.* **9**, 967–986 (1985).
13. Nissen, K. K., Vogel, U. & Nexo, B. A. Association of a single nucleotide polymorphic variation in the human chromosome 19q13.3 with drug responses in the NCI60 cell lines. *Anticancer Drugs* **20**, 174–178 (2009).
14. Hashizume, C. *et al.* Nucleoporin Nup62 maintains centrosome homeostasis. *Cell Cycle* **12**, 3804–3816 (2013).
15. Garnett, M. J. *et al.* UBE2S elongates ubiquitin chains on APC/C substrates to promote mitotic exit. *Nat. Cell Biol.* **11**, 1363–1369 (2009).
16. Clarke, C. *et al.* Correlating transcriptional networks to breast cancer survival: a large-scale coexpression analysis. *Carcinogenesis* **34**, 2300–2308 (2013).
17. Zheng, X. *et al.* Cnot1, Cnot2, and Cnot3 maintain mouse and human ESC identity and inhibit extraembryonic differentiation. *Stem Cells* **30**, 910–922 (2012).
18. Chiyoda, T. *et al.* Expression profiles of carcinosarcoma of the uterine corpus-are these similar to carcinoma or sarcoma. *Genes Chromosomes Cancer* **51**, 229–239 (2012).
19. Mohr, S. *et al.* Microdissection, mRNA amplification and microarray: a study of pleural mesothelial and malignant mesothelioma cells. *Biochimie* **86**, 13–19 (2004).
20. Fernandez-Ranvier, G. G. *et al.* Identification of biomarkers of adrenocortical carcinoma using genomewide gene expression profiling. *Arch. Surg.* **143**, 841–846; discussion 846 (2008).
21. Syed Ikmal, S. I., Zaman Huri, H., Vethakkan, S. R. & Wan Ahmad, W. A. Potential biomarkers of insulin resistance and atherosclerosis in type 2 diabetes mellitus patients with coronary artery disease. *Int. J. Endocrinol.* **2013**, 698567 (2013).
22. Bartholin, L. *et al.* TGIF inhibits retinoid signaling. *Mol Cell Biol.* **26**, 990–1001 (2006).
23. Hamid, R. & Brandt, S. J. Transforming growth-interacting factor (TGIF) regulates proliferation and differentiation of human myeloid leukemia cells. *Mol. Oncol.* **3**, 451–463 (2009).
24. Hamid, R., Patterson, J. & Brandt, S. J. Genomic structure, alternative splicing and expression of TG-interacting factor, in human myeloid leukemia blasts and cell lines. *Biochim. Biophys. Acta.* **1779**, 347–355 (2008).
25. Reynolds, C. P. *et al.* Retinoic-acid-resistant neuroblastoma cell lines show altered MYC regulation and high sensitivity to fenretinide. *Med. Pediatr. Oncol.* **35**, 597–602 (2000).
26. Leopoldino, A. M. *et al.* SET protein accumulates in HNSCC and contributes to cell survival: antioxidant defense, Akt phosphorylation and AVOs acidification. *Oral Oncol.* **48**, 1106–1113 (2012).
27. Saraon, P. *et al.* Evaluation and prognostic significance of ACAT1 as a marker of prostate cancer progression. *Prostate* **74**, 372–380 (2014).
28. Bemlih, S., Poirier, M. D. & El Andaloussi, A. Acyl-coenzyme A: cholesterol acyltransferase inhibitor Avasimibe affect survival and proliferation of glioma tumor cell lines. *Cancer Biol. Ther.* **9**, 1025–1032 (2010).
29. Chi, J. H. *et al.* Increased expression of the glioma-associated antigen ARF4L after loss of the tumor suppressor PTEN. Laboratory investigation. *J. Neurosurg.* **108**, 299–303 (2008).
30. Tanabe, S. *et al.* AF10 is split by MLL and HEAB, a human homolog to a putative Caenorhabditis elegans ATP/GTP-binding protein in an invins(10;11)(p12;q23q12). *Blood* **88**, 3535–3545 (1996).
31. Edwards, H. *et al.* RUNX1 regulates phosphoinositide 3-kinase/AKT pathway: role in chemotherapy sensitivity in acute megakaryocytic leukemia. *Blood* **114**, 2744–2752 (2009).
32. Kilbey, A. *et al.* Runx regulation of sphingolipid metabolism and survival signaling. *Cancer Res.* **70**, 5860–5869 (2010).
33. Jia, R., Li, C., McCoy, J. P., Deng, C. X. & Zheng, Z. M. SRp20 is a proto-oncogene critical for cell proliferation and tumor induction and maintenance. *Int. J. Biol. Sci.* **6**, 806–826 (2010).

34. Roberts, J. M. *et al*. Splicing factor TRA2B is required for neural progenitor survival. *J. Comp. Neurol.* **522**, 372–392 (2014).
35. Craggs, T. D., Hutton, R. D., Brenlla, A., White, M. F. & Penedo, J. C. Single-molecule characterization of Fen1 and Fen1/PCNA complexes acting on flap substrates. *Nucleic Acids Res.* **42**, 1857–1872 (2014).
36. Sandhu, S. K., Yap, T. A. & de Bono, J. S. The emerging role of poly(ADP-Ribose) polymerase inhibitors in cancer treatment. *Curr. Drug Targets* **12**, 2034–2044 (2011).
37. Lord, C. J. & Ashworth, A. Mechanisms of resistance to therapies targeting BRCA-mutant cancers. *Nat. Med.* **19**, 1381–1388 (2013).
38. Sakamoto, M. *et al.* Analysis of gene expression profiles associated with cisplatin resistance in human ovarian cancer cell lines and tissues using cDNA microarray. *Hum. Cell* **14**, 305–315 (2001).
39. Kim, S. H. *et al.* Ku autoantigen affects the susceptibility to anticancer drugs. *Cancer Res.* **59**, 4012–4017 (1999).
40. Kim, S. H. *et al.* Potentiation of chemosensitivity in multidrug-resistant human leukemia CEM cells by inhibition of DNA-dependent protein kinase using wortmannin. *Leuk. Res.* **24**, 917–925 (2000).
41. Schneider, J., Centeno, M., Jimenez, E., Rodriguez-Escudero, F. J. & Romero, H. Correlation of MDR1 expression and oncogenic activation in human epithelial ovarian carcinoma. *Anticancer Res.* **17**, 2147–2151 (1997).
42. Yokoyama, A. *et al*. Differentiation inhibitory factor nm23 as a new prognostic factor in acute monocytic leukemia. *Blood* **88**, 3555–3561 (1996).
43. An, R. *et al*. Over-expression of nm23-H1 in HeLa cells provides cells with higher resistance to oxidative stress possibly due to raising intracellular p53 and GPX1. *Acta. Pharmacol. Sin.* **29**, 1451–1458 (2008).
44. Weeks, L. D., Fu, P. & Gerson, S. L. Uracil-DNA glycosylase expression determines human lung cancer cell sensitivity to pemetrexed. *Mol. Cancer Ther.* **12**, 2248–2260 (2013).
45. Li, L., Monckton, E. A. & Godbout, R. A role for DEAD box 1 at DNA double-strand breaks. *Mol. Cell Biol.* **28**, 6413–6425 (2008).
46. Mosmann, T. Rapid colorimetric assay for cellular growth and survival: application to proliferation and cytotoxicity assays. *J. Immunol. Methods* **65**, 55–63 (1983).
47. Guan, X. Y. *et al*. Recurrent chromosome alterations in hepatocellular carcinoma detected by comparative genomic hybridization. *Genes Chromosomes Cancer* **29**, 110–116 (2000).
48. Wang, J. *et al.* 1p31, 7q21 and 18q21 chromosomal aberrations and candidate genes in acquired vinblastine resistance of human cervical carcinoma KB cells. *Oncol. Rep.* **19**, 1155–1164 (2008).
49. Wang, J. *et al*. Transcriptional analysis of doxorubicin-induced cytotoxicity and resistance in human hepatocellular carcinoma cell lines. *Liver Int.* **29**, 1338–1347 (2009).

Acknowledgments

The work described in this paper was supported by the National Natural Science Foundation of China 81271919.

Author contributions

Conceived and designed the experiments: J.W., S.M.L. Performed the experiments: J.W., S.M.L. Analyzed the data: W.C., J.W. Contributed reagents/materials/analysis tools: S.M.L., W.C. Wrote the manuscript: J.W., S.M.L.

Additional information

Supplementary information accompanies this paper at http://www.nature.com/scientificreports

Competing financial interests: The authors declare no competing financial interests.

How to cite this article: Liu, S.-M., Chen, W. & Wang, J. Distinguishing between cancer cell differentiation and resistance induced by all-trans retinoic acid using transcriptional profiles and functional pathway analysis. *Sci. Rep.* **4**, 5577; DOI:10.1038/srep05577 (2014).